# Effect of alkaline-earth and transition metals on the electrical transport of double perovskites

A. Poddar, S. Das, and B. Chattopadhyay

Citation: Journal of Applied Physics **95**, 6261 (2004); doi: 10.1063/1.1728294
View online: http://dx.doi.org/10.1063/1.1728294
View Table of Contents: http://scitation.aip.org/content/aip/journal/jap/95/11?ver=pdfcov
Published by the AIP Publishing



# Effect of alkaline-earth and transition metals on the electrical transport of double perovskites

A. Poddar,[a] S. Das, and B. Chattopadhyay[b]
*Saha Institute of Nuclear Physics I/AF, Bidhannagar, Calcutta-700 064, India*

(Received 10 July 2003; accepted 7 March 2004)

The transport properties of $A_2BMoO_6$ ($A$=Ca, Sr, and Ba; $B$=Cr, Mn, and Fe) crystals are investigated from studies of x-ray diffraction, thermoelectric power (TEP) $S$, and resistivity $\rho$ measurements over a wide temperature range (20–900 K). The resistivity of $A_2FeMoO_6$ ($A$=Ca, Sr, and Ba) crystals shows a metallic character and its analysis suggests that the electron-electron scattering is one of the contributions governing the conduction mechanism of these compounds. On the other hand, $Ca_2MnMoO_6$ shows an insulator-metal transition similar to that reported in rare earth nickelate [Phys. Rev. B **45**, 8209 (1992)]. The conductivity $\sigma(T)$ data of $Sr_2CrMoO_6$ can be best fitted in terms of simultaneous contributions to $\sigma$ with an activated-type process and variable range hopping (VRH) mechanism. In the case of $Sr_2MnMoO_6$, $\rho(T)$ behavior follows an activated-type hopping for $T>400$ K whereas for $T<85$ K it can be described satisfactorily by VRH mechanism. For all the compounds, TEP exhibits negative values ($n$ type) except for $Ca_2FeMoO_6$ which shows a crossover from positive ($p$ type) to negative values ($n$ type) around $T=147$ K. From the metallic diffusion part of TEP, Fermi energy $E_F$ is estimated to be 0.86 eV, 1.2 eV, and 0.8 eV for $Sr_2FeMoO_6$, $Ca_2FeMoO_6$, and $Ca_2MnMoO_6$, respectively. © *2004 American Institute of Physics.* [DOI: 10.1063/1.1728294]

## I. INTRODUCTION

Recently strongly correlated electron systems with a half metallic character, i.e., compounds with only one spin direction at the Fermi level ($E_F$), have attracted considerable attention[1,2] both from fundamental and practical points of view. Because of the high spin polarization inherent to these oxides carrier motion depends sensitively on the relative angles between their magnetic moments that can be controlled by a low magnetic field. In this sense, half metallic oxides with high magnetic transition temperature close to room temperature with spin dependent transport are the promising candidates for technological application.[3] In case of half metallic manganites, the intergrain magnetoresistance (MR) becomes smaller as $T_C$ increases to room temperature and restricts their use in magnetoresistive devices. Very recently observation[4] of low field MR at room temperature in the double perovskite metallic $Sr_2FeMoO_6$ (SFMO) compound is found to be appropriate for the purpose because of the material's high value for $T_C$ (~400 K). Besides the technological importance substantial research efforts have also been devoted to understand the electronic and magnetic properties of the double-perovskite compounds $A_2B'B''O_6$ (Ref. 5) where $A$ is 12-fold coordinated alkaline-earth metal ion and $B'$,$B''$ are transition metal ions with sixfold coordination with oxygen. Depending upon the amount of the Fe and Mo atoms the crystal symmetry of ordered SFMO is found to be cubic or tetragonal where each of the $Fe^{3+}$ and $Mo^{5+}$ sublattices is considered to be ferromagnetically ordered while the two sublattices are coupled to each other antiferromagnetically.[6,7] The ferrimagnetism of this compound has been ascribed to the antiferromagnetic superexchange interaction between $Mo^{5+}$ ($4d^1$) spin and $Fe^{3+}$ ($3d^5$) spin leading to a saturation magnetization $M_S=4\mu_B$. This value for $M_S$ is irrespective of the valence degeneracy of the cations at the $B'$ and $B''$ sites (viz. $Fe^{3+}+Mo^{5+}=Fe^{2+}+Mo^{6+}$) and is slightly higher compared to the value $M_S=3.4\mu_B$ observed experimentally. This descrepancy is believed to arise from the mis-site disorder of Fe sites by Mo species and vice versa. It is to be mentioned here that for $Fe^{2+}$-$Mo^{6+}$ combination there exists no local magnetic moment at the Mo site. A density functional calculation[4] has shown that the occupied up-spin band mainly composed of $Fe^{3+}$ electrons is separated by a gap from the Fermi level lying in the down-spin band consisting of Fe $t_{2g}$ and Mo $t_{2g}$ electrons. Consequently, charge carriers are almost spin polarized at $E_F$ giving rise to half metallic character.[4,8,9] Thus the electrons of Fe and Mo may behave as localized and itinerant, respectively. The observed metallicity and magnetic properties of SFMO can be explained considering the valence degeneracy of the cations at $B'$ and $B''$ sites as proposed by Sleight and Weiher.[10] This is also supported by the electronic structure calculation which shows that at the Fermi level down-spin Mo $4d$ $t_{2g}$, Fe $3d$ $t_{2g}$, and $O_{2p}$ states are mixed up and form narrow conduction band, and provide conduction mechanism. In contrast, $Sr_2MnMoO_6$ which belongs to the same double-perovskite family shows insulating property[11] as it contains no Mo $4d$ electrons responsible for metallic conductivity. The insulating property along with antiferromagnetic ordering ($T_N=16-37$ K) has also been observed[12–14] in another member $Sr_2FeWO_6$ of the above family. Here, all the W atoms are in the $W^{6+}$ state and con-

[a]Electronic address: poddar@cmp.saha.ernet.in
[b]Present address: Lady Brabourne College, P1/2 Suhrawardy Avenue, Calcutta-700 017, India

 

sequently Fe atoms adopt the $Fe^{2+}$ state giving rise to insulating property as a result of complete localization of the valence electrons. A transition from ferrimagnetic metal to antiferromagnetic insulator has been reported[15–17] in $Sr_2Fe(Mo_{1-x}W_x)O_6$ for composition around the critical concentration $x \sim 0.25$. The authors interpreted the metal-insulator (MI) transition in terms of valence fluctuation between $Fe^{2+}/(W,Mo)^{6+}$ and $Fe^{3+}/(W,Mo)^{5+}$ due to the stability of the $Mo^{5+}$ valence or, more plausibly, the percolation model. In this system the thermopower $S$ as a function of $x$ shows a change from $p$ type to $n$ type with increasing temperature at $T_{np}$ that changes monotonically with $x$ for the range $0.2 \leqslant x \leqslant 0.75$.[16] Thus it is clear that the nature of transition metals at $B'$ and $B''$ sites of the double perovskite $A_2B'B''O_6$ plays an important role for the conduction process. Here we have systematically studied the electrical resistivity and thermoelectric power (TEP) $S$ of the double-perovskite $A_2BMoO_6$ single crystals where $A$ = Ca, Sr, and Ba and $B$ = Cr, Mn, and Fe in order to understand the conduction mechanism, thereby throwing some light on the nature of MI transition, if exists, on these crystals.

## II. EXPERIMENT

Single crystalline $A_2BMoO_6$ ($A$ = Ca, Sr, and Ba and $B$ = Cr, Mn, and Fe) was melt grown by the floating zone method. For the preparation of bulk $A_2BMoO_6$ material corresponding to the above composition stoichiometric amounts of $ACO_3$ ($A$ = Ca, Sr, and Ba), $Fe_2O_3$, $Cr_2O_3$, MnO, and $MoO_3$ were mixed, ground, and calcined at 1000 °C in a flow of 1:9 ratio of $H_2$ and Ar gas mixture for 6 h with intermediate grindings. Finally, the mixture was well ground, pressed into pellets, and sintered at about 1270 °C for 2 h in a flow of 1:9 ratio of $H_2$ and Ar gas mixture. The structures for each of the above composition were confirmed by x-ray diffraction. Then pellets were crushed, pulverized to powder, and pressed into rods of dimensions $5 \times 80$ mm$^2$ and finally sintered at 1270 °C for 1 h in the same gaseous atmosphere. Using traveling solvent floating zone (TSFZ) image furnace all the crystals were grown at a feeding speed of 20–30 mm/h in Ar atmosphere. Black and shiny crystals of size 4 mm in diameter and 10 mm in length were obtained. For the better ordering of Fe and Mo all the as-grown $A_2BMoO_6$ crystals were annealed at 1250 °C for 12 h in a flow of $H_2$ and Ar gas mixture (in the ratio 1:9) and then cooled at the rate of 50 °C/h to room temperature. All the subsequent experiments were performed on these annealed samples.

The crystal structure and the phase purity of each of the crystals were checked by the powder x-ray diffraction with Cu $K\alpha$ radiation using the Philips APD1877 x-ray diffractometer. The dc electrical resistivity measurements were performed following four-probe technique. The thermopower of the samples was measured using a differential technique. The details of the setup and measurement technique have been reported earlier.[18]

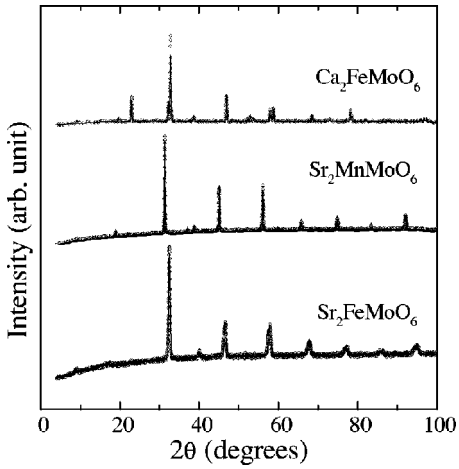


FIG. 1. X-ray diffraction patterns for $A_2FeMoO_6$ ($A$ = Ca and Sr) and $Sr_2MnMoO_6$ single crystals.

## III. RESULTS AND DISCUSSION

### A. X-ray diffraction

The quality of the samples and their crystallographic structure have been investigated by means of room-temperature powder x-ray diffraction technique. Figure 1 presents the x-ray diffraction spectrum of some double-perovskite samples. The patterns were obtained taking the diffraction picture by step-scanning procedure for the powder sample obtained by grinding the single crystal grown by TSFZ image furnace. No traces of impurities were detected in the x-ray diffraction pattern. The analysis of the x-ray spectrum for $Sr_2FeMoO_6$, $Sr_2MnMoO_6$, and $Sr_2CrMoO_6$ is found to be consistent with tetragonal symmetry ($I4/mmm$) although the diffraction profiles (Fig. 1) for $Sr_2FeMoO_6$ and $Sr_2MnMoO_6$ do not contain double peaks. This could be due to disorder or internal strains. The structural parameters are summarized in Table I. The observed tetragonal symmetry of $Sr_2FeMoO_6$ at room temperature is in agreement with the results reported by Moritomo *et al.*[6] The authors[6] observed that the crystal structure of the compound is cubic ($Fm\bar{3}m, Z=4$) in the paramagnetic phase while that in the

TABLE I. Structural parameters of $A_2BMoO_6$ ($A$ = Ca, Sr, Ba and $B$ = Cr, Mn, Fe).

| Sample | Symmetry | $a$ (Å) | $b$ (Å) | $c$ (Å) | $\beta$ |
|---|---|---|---|---|---|
| $Ca_2FeMoO_6$ | $P2_1/n$ | 5.4165 ± 0.0003 | 5.5392 ± 0.0003 | 7.7152 ± 0.0003 | 89.927 ± 0.0035 |
| $Ca_2MnMoO_6$ | $P2_1/n$ | 5.4145 ± 0.0002 | 5.5149 ± 0.0002 | 7.7818 ± 0.0003 | 89.913 ± 0.0035 |
| $Sr_2FeMoO_6$ | $I4/mmm$ | 5.5447 ± 0.0002 | | 7.8393 ± 0.0003 | |
| $Sr_2MnMoO_6$ | $I4/mmm$ | 5.6505 ± 0.0002 | | 7.9987 ± 0.0004 | |
| $Sr_2CrMoO_6$ | $I4/mmm$ | 5.5688 ± 0.0003 | | 7.9054 ± 0.0003 | |
| $Ba_2FeMoO_6$ | $Fm\bar{3}m$ | 8.0686 ± 0.0002 | | | |

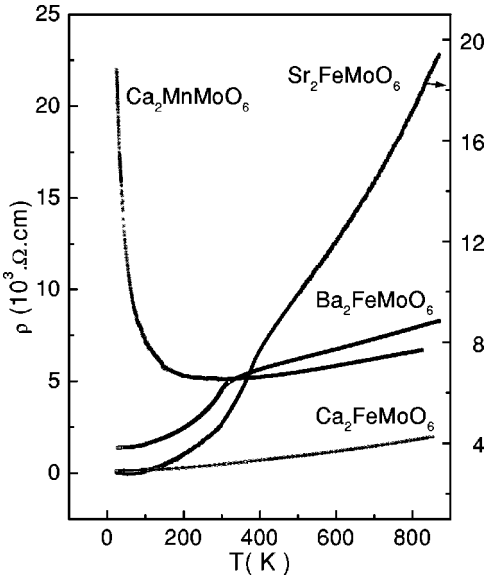


FIG. 2. The temperature dependence of resistivity of $A_2FeMoO_6$ ($A$=Ca, Sr, and Ba) and $Ca_2MnMoO_6$ crystals.

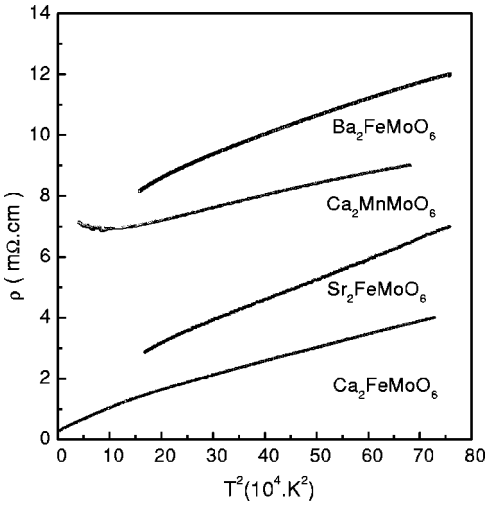


FIG. 3. The temperature variation of resistivity as a function of $T^2$ for $A_2FeMoO_6$ ($A$=Ca, Sr, and Ba) and $Ca_2MnMoO_6$ crystals.

ferrimagnetic phase is tetragonal ($I4/mmm, Z=2$). For $Ca_2FeMoO_6$ and $Ba_2FeMoO_6$ crystals we observed that the x-ray diffraction peaks can be indexed successfully considering monoclinic ($P2_1/n$) and cubic ($Fm\bar{3}m$) structures, respectively. Borges *et al.*[7] have also observed that the x-ray diffraction data for $A_2FeMoO_6$ ($A$=Ca, Sr, and Ba) can be indexed quite consistently with monoclinic, tetragonal, and cubic symmetries, respectively. In addition to this, our x-ray results for $A_2FeMoO_6$ ($A$=Ca, Sr, and Ba) are consistent with the x-ray Rietveld analysis results performed by Ritter *et al.*[19,20] for the same compounds. It is to be mentioned here that the knowledge of tolerance factor $t$ determines the crystal structure of perovskite $ABO_3$. The reported crystal structures of $A_2FeMoO_6$ ($A$=Ca, Sr, and Ba) as a function of $t$ are as follows: $Ca_2FeMoO_6$ with $t=0.954$ is found to be monoclinic, or tetragonal, while $Sr_2FeMoO_6$ with $t=1.009$ is almost cubic, and $Ba_2FeMoO_6$ with $t=1.06$ is cubic. The emperical rule formulated by Philipp *et al.*[21] is that when $t$ satisfies $0.96 \leqslant t \leqslant 1.06$ the majority of the double perovskites are found to be cubic/tetragonal and for $t \leqslant 0.96$ they belong to orthorhombic, or monoclinic, structures while for $1.06 \leqslant t$ a hexagonal structure is favored.

### B. Resistivity

The transport properties of all the single-crystal samples are investigated over a broad temperature range extending from 20 K to 900 K. The crystals show high conductivity because they contain few grain boundaries than the polycrystalline ones. Figure 2 shows the temperature variation of resistivity $\rho$ of $A_2FeMoO_6$ ($A$=Ca, Sr, and Ba) and $Ca_2MnMoO_6$ crystals. For $A_2FeMoO_6$, $\rho(T)$ shows a metallic behavior ($d\rho/dT>0$) throughout the temperature range studied. The electronic structure of $Sr_2FeMoO_6$ shows that a gap is formed in spin-up density of states (DOS) at the Fermi level $E_F$ whereas there is a finite and continuous down-spin DOS across $E_F$. This implies that the majority spin electrons are insulating whereas the minority spin electrons are metallic thereby producing fully spin polarized conduction electrons at $E_F$. This will give rise to a half metallic ground state for $Sr_2FeMoO_6$. The electronic structure of $Ba_2FeMoO_6$ (Ref. 22) is similar to that of $Sr_2FeMoO_6$ and also shows a half metallic nature. The $\rho(T)$ curves of these two compounds exhibit almost similar nature. The resistivity value of $Ca_2FeMoO_6$ is found to be smallest compared to those of SFMO and BFMO. The electrical conductivity of $Ca_2MnMoO_6$ is metallic at room temperature and above but it undergoes a transition around 209 K to an insulating state, i.e., a sharp insulator-metal (IM) transition is observed which is absent in all other double-perovskite crystals studied here. Such a sharp IM transition has also been observed[23] in $RNiO_3$ where the rare earth $R$ stands for Pr, Nd, and Sm.

In Fig. 3 we have shown the variation of the resistivity as a function of $T^2$ for $A_2FeMoO_6$ ($A$=Ca, Sr, and Ba) and $Ca_2MnMoO_6$ crystals. For $Ca_2FeMoO_6$, Fig. 3 shows that the resistivity is proportional to $T^2$ throughout the measured temperature interval studied. In the case of $Ca_2MnMoO_6$, $\rho$ scales well with $T^2$ nature in the high temperature range but in the low temperature insulating region it deviates from the $T^2$ behavior. For $Sr_2FeMoO_6$, however, $\rho$ versus $T^2$ curve follows two straight lines with different slopes. Deviations occur around the transition temperature. This observation indicates that electron-electron scattering,[6,24] or electron-magnon scattering,[25] controls the behavior of resistivity of these compounds. Enhancement of the electron-spin scattering component brings about a deviation from the $T^2$ law of the $\rho(T)$ curve near about $T_C$. On the other hand, in the high temperature region, $\rho(T)$ of $Ba_2FeMoO_6$ is found to vary linearly with $T$ similar to an ideally pure metal.

Figures 4(a) and 4(b) depict the insulating nature of $Sr_2MnMoO_6$ and $Sr_2CrMoO_6$ crystals. Though the $\rho(T)$ curve of $Sr_2MnMoO_6$ shows an insulating behavior it is marked with a hump near about 219 K [Fig. 4(a)]. The insulating nature of $Sr_2MnMoO_6$ can be attributed to the absence of the $4d^1$ electrons in the hexavalent $Mo^{6+}$ ($4d^0$) ions. This is also consistent with the paramagnetic behavior of the

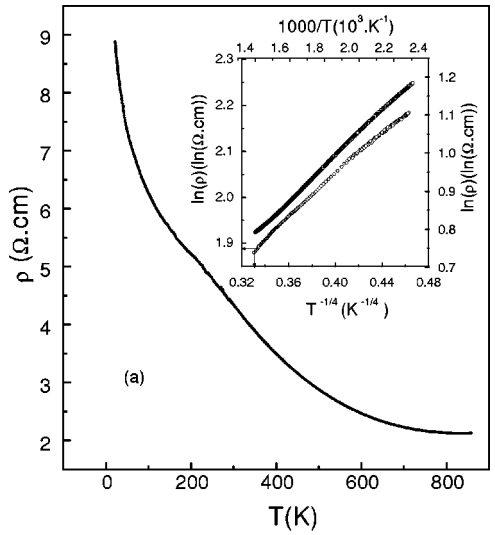


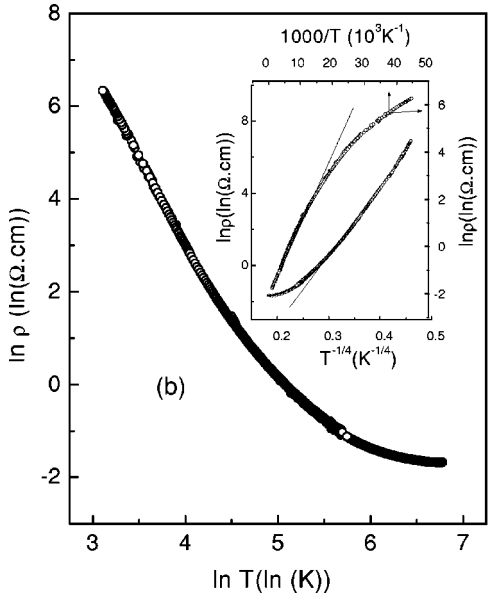


FIG. 4. (a) The resistivity of $Sr_2MnMoO_6$ as a function of temperature. The inset shows the ln $\rho$ against $1000/T$ and ln $\rho$ against $1/T^{1/4}$ dependences. (b) Plot of ln $\rho$ as a function of ln $T$ for $Sr_2CrMoO_6$ crystal. The inset shows the ln $\rho$ against $1000/T$ and ln $\rho$ against $1/T^{1/4}$ dependences.

compound.[26] Figure 4(b) shows that the electrical transport of $Sr_2CrMoO_6$ with a tetragonal crystal structure behaves like an insulating material. For the insulating oxide samples, usually it has been observed that at low temperature electrical conduction behavior can be described by a very low density of localized states produced by impurities, disorder, etc. within the band gap region. In this region, Mott's variable range hopping (VRH) mechanism[27] accounts satisfactorily the temperature dependent electrical transport, following the expression

$$\sigma = \sigma_{01} \exp[-(T_0/T)^{1/4}]. \quad (1)$$

On the other hand, at high temperature the conduction takes place by the thermally activated hopping of the charge carriers across the band gap according to the expression[28]

$$\sigma = \sigma_{02} \exp[-E_q/2k_BT], \quad (2)$$

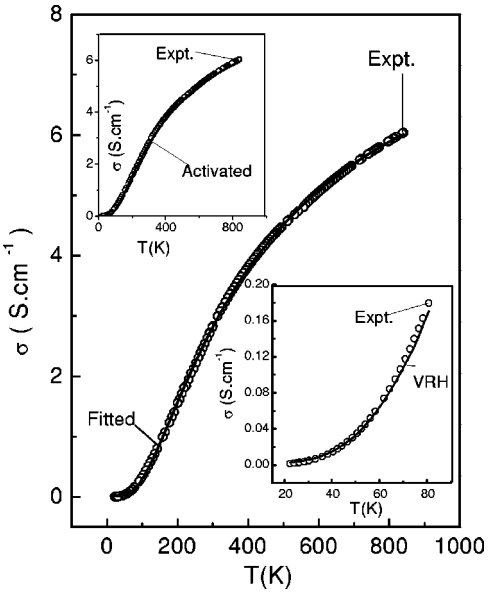


FIG. 5. The electrical conductivity (open circles) of $Sr_2CrMoO_6$ crystal as a function of temperature. The solid line shows the best fit. The contributions from the activated component and the VRH component are shown in the insets.

where $\sigma_{01}$ and $\sigma_{02}$ are constants, and $T_0$ and $E_g$ are the Mott temperature and the activation energy, respectively.

It has already been mentioned that the end member $Sr_2FeWO_6$ of $Sr_2Fe(Mo_{1-x}W_x)O_6$ series exhibits insulating property due to the complete localization of the valence electrons. In order to analyze the conductivity data of the insulating $Sr_2FeWO_6$ Roy *et al.*[17] found that the transport does not follow a single activated dependence over the entire temperature range. However, the authors found that the experimental data can be best fitted in terms of simultaneous contributions to the conductivity ($\sigma$) both by an activated process [Eq. (2)] and variable range hopping [Eq. (1)]. Maiti *et al.*[29] have also observed that the insulating behavior of $La_{1-x}Ca_xVO_3$ ($x=0$ and 0.1) compound can be described satisfactorily following the above mentioned procedure. We have also found that the resistivity data of the insulating $Sr_2CrMoO_6$ crystal cannot be described by a single activated dependence as illustrated in the insets [Fig. 4(b)], where we show the dependence of ln $\rho$ against $1000/T$. The insets show a simple activated behavior at the high temperature regime. In the low temperature region the conduction is best described by the VRH mechanism as illustrated in the insets by the linear dependence of ln $\rho$ on $T^{-1/4}$. However, following the fitting procedure of Roy *et al.*[17] we have found that the experimental conductivity data over the whole temperature range can be fitted in a best way by combining the contributions to $\sigma(T)$ due to an activated hopping process, Eq. (2), and that of VRH mechanism, Eq. (1), i.e., following the expression

$$\sigma = \sigma_{01} \exp[-E_g/2k_BT] + \sigma_{02} \exp[-(T_0/T)^{1/4}]. \quad (3)$$

In Fig. 5 we have shown the best fit to the conductivity of $Sr_2CrMoO_6$ crystal in terms of expression (3) for $\sigma(T)$ as a solid line through the experimental data points (open circles). The fitting provides an activation energy of 0.1 eV

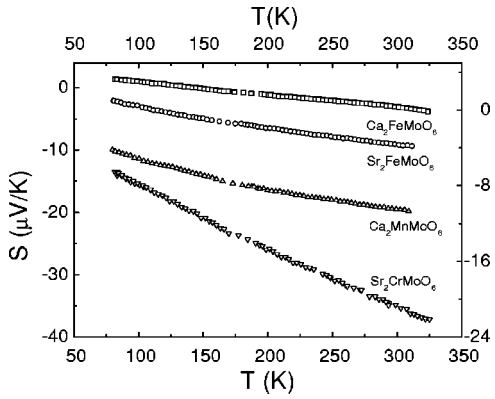


FIG. 6. Variation of thermopower $S$ of $Sr_2FeMoO_6$, $Ca_2FeMoO_6$, $Ca_2MnMoO_6$, and $Sr_2CrMoO_6$ crystals with temperature.

which matches exactly with the gap value of 0.1 eV obtained from optical spectroscopic[11] measurements. The contribution of the activated as well as that of VRH term to $\sigma(T)$ are also marked in the insets of the figure. It is clear from the figure that the activated behavior dominates over the VRH contribution throughout the temperature range except for at the low temperatures. It should be mentioned here that in systems with localized carriers, with increasing temperature there exists a crossover from VRH to nearest neighbor hopping. It is noteworthy that in double-perovskite oxides such as $Sr_2CrMoO_6$, $Sr_2FeWO_6$ and perovskite oxides such as $La_{1-x}Ca_xVO_3$ ($x=0$ and 0.1) the combination of variable range and activated contributions to the conductivity fits the experimental data quite satisfactorily.

Although the electrical transport behavior of $Sr_2MnMoO_6$ crystal is found to be insulating in nature [Fig. 4(a)] but due to the presence of a small hump at 219 K, its nature of $\rho(T)$ or $\sigma(T)$ over the entire range of temperature cannot be explained by the above mentioned method. Insets of Fig. 4(a) show the linear dependence of $\ln\rho$ with $1000/T$ leading to a simple activated behavior at the high temperature region (440–700 K) whereas in the low temperature regime, the electrical transport can be best described by the VRH mechanism, as illustrated in the insets by the linear variation of $\ln\rho$ with $T^{-1/4}$.

### C. Thermoelectric power

The thermoelectric power $S$ is a zero current transport coefficient and is a very useful probe to study the semiconducting and metallic behavior of compounds since it offers a characteristic difference in the two cases. The metallic TEP in these compounds has a low value at room temperature and varies linearly with temperature. The sign of the TEP describes (not always) the type of majority carriers present in the compound at a certain temperature.

Figure 6 shows the thermal variation of $S$ for $A_2FeMoO_6$ ($A=$Ca and Sr), $Ca_2MnMoO_6$, and $Sr_2CrMoO_6$ crystals. All the double-perovskite crystals studied here show negative values for $S$ at room temperature indicating electronic conduction. The variation of $S(T)$ for $Sr_2FeMoO_6$ behaves like a typical $n$-type metal with a linear temperature dependence consistent with its $\rho(T)$ behavior. It is to be mentioned here that perfectly ordered $Sr_2FeMoO_6$ has threefold degenerate minority spin $\pi^*$ bands whose one-sixth filling gives rise to a $n$-type metallic behavior. A similar metallic variation of $S$ with $T$ along with a crossover from positive ($p$ type) to negative ($n$ type) $S$ has been observed in $Ca_2FeMoO_6$ crystal. Figure 6 also depicts that for $Ca_2MnMoO_6$, $S$ varies linearly with $T$ only in the high temperature side and at low temperature it starts deviating from the linear dependence consistent with its $\rho(T)$ behavior. In the same figure we have also shown the variation of $S(T)$ with $T$ for $Sr_2CrMoO_6$ crystal. Figure shows that the temperature dependence of $S$ is quite linear similar to that observed in $Ca_2MnMoO_6$ crystal which follows metallic transport at high temperature. Although $Sr_2CrMoO_6$ crystal exhibits insulatinglike behavior in $\rho(T)$ in the temperature interval $75\ \mathrm{K}<T<300\ \mathrm{K}$ its resistivity value is comparable to that of metals. The observed linear dependence of $S(T)$ over the temperature interval studied may be due to its lower values of resistivity. On the other hand, in the case of more insulating $Sr_2MnMoO_6$ crystal we have found large negative values for $S$ which are not reliable.

It is to be pointed out here that monovalent metals, noble metals, and some other metals[30] also exhibited linear dependence of $S$ on $T$ similar to that observed in double-perovskite oxides mentioned above. Considering the nearly free electron model Mott[31] has given an expression for the characteristic diffusion thermopower of a metal as

$$S(T)=(\pi^2k_B^2T/3e)[d[\ln\sigma(E)]/dT]_{E=E_F}, \tag{4}$$

where $k_B$ is the Boltzmann's constant, $E_F$ is the Fermi energy, and $e$ is the charge of the carriers. Assuming that the conductivity is proportional to the energy and that there is a $T$-independent mean free path for the carriers, the expression (4) becomes

$$S(T)\approx\pi^2k_B^2T/3eE_F. \tag{5}$$

Equation (5) is derived considering a spherical Fermi surface together with a $T$-independent relaxation. This approximation limits the validity of Eq. (5) at low temperature. From the above relation $S$ is linear with $T$ and is extremely sensitive to the nature of the Fermi surface. The small linear contribution to the thermopower reflects the highly conductive metallic character within the compound. From the slope of $S(T)$ and using the relation (5), we have estimated Fermi energies $E_F=0.86$ eV, 1.2 eV, and 0.8 eV for $Sr_2FeMoO_6$, $Ca_2FeMoO_6$, and $Ca_2MnMoO_6$ crystals, respectively.

In Fig. 7 we have presented the thermal variation of $S$ for BFMO crystal. Figure shows that the variation of $S(T)$ is parabolic in nature and passes through a minima around 197 K. This feature of $S$ is quite different from that of all the double perovskites studied here. In case of transition metals the thermal variation of $S$ is often marked by peculiar features such as maxima, minima, bending, reversal of sign, etc. In most of the cases, the $S$ versus $T$ curve shows deviation from the linear behavior due to electron-phonon, electron-magnon scattering, complicated band structure, impurity scattering, etc. At low temperatures, the contribution in $S$ due to the scattering of electrons with phonons giving rise to a phonon-drag effect is found to be proportional to the lattice specific heat. Hence, the phonon-drag contribution $S_g$ in $S$

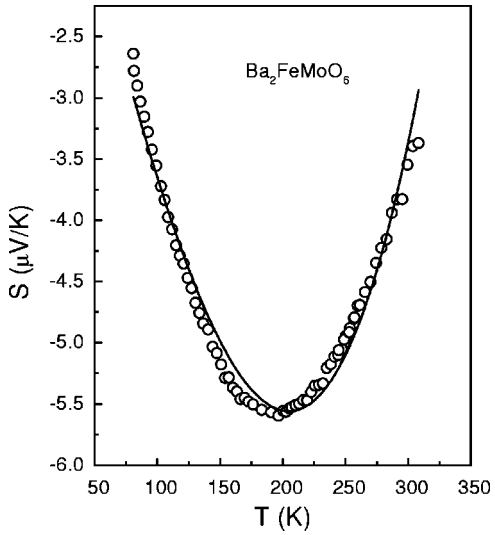


FIG. 7. The temperature dependence of the thermopower $S$ for $Ba_2FeMoO_6$. Solid line is the theoretical fit to the experimental data following the relation $S(T)=S_0+S_1T+S_2T^3$.

can be expressed as $S_g \sim T^3$. We have found that the thermopower data of the BFMO single crystal can be fitted quite satisfactorily considering the following expression for $S(T)$:

$$S(T)=S_0+S_1T+S_2T^3. \tag{6}$$

Here, $S_0$ ($S$ at $T=0$) can be obtained from the extrapolation of the high temperature fit of $S$. This term has no physical origin and is inserted to overcome the problem of truncating the low temperature data. The $T$-linear term may arise from the metallicity of the crystal while the third term represents the phonon drag contribution in $S$. Although measured $S(T)$ data (77–325 K) fit (solid line) well with the expression (6), however, the presence of minima in the measured $S(T)$ data around $T=200$ K is not due to the phonon drag effect as it appears only at low temperatures. In order to elucidate the true origin of minima further experimental data from varieties of experiments are needed.

## IV. CONCLUSION

The results presented in this work are summarized as follows.

(1) For $A_2FeMoO_6$ ($A=$Ca, Sr, and Ba) crystals, the crystallographic structure changes from cubic ($A=$Ba) to tetragonal ($A=$Sr) and finally to monoclinic ($A=$Ca) with the decrease of the average ionic radius. The resistivity of $A_2FeMoO_6$ upholds a metallic character and is found to vary linearly with $T^2$. This behavior is reminiscent of the electron-electron or electron-magnon scattering.

(2) $Ca_2MnMoO_6$ is metallic (M) in the high temperature region and insulating (I) in the low temperature region thereby giving rise to an IM transition similar to that found in $RNiO_3$ ($R=$Pr, Nd, Sm). The metallic part of $\rho(T)$ also follows $T^2$ dependence.

(3) $Sr_2CrMoO_6$ and $Sr_2MnMoO_6$ are insulating in nature. The low temperature insulating behavior can be explained in the light of VRH mechanism whereas at elevated temperatures activated type hopping is found to be operative. The conductivity $\sigma(T)$ data of $Sr_2CrMoO_6$ can be best fitted over the whole temperature range taking into account simultaneous contributions to $\sigma$ with an activated type process and VRH mechanism.

(4) The double perovskites studied here offer negative sign for the TEP over the whole thermal range except for $Ca_2FeMoO_6$ which exhibits a crossover in $S$ around $T=147$ K. The Fermi energy $E_F$ estimated from the linear part of $S$ for $A_2FeMoO_6$ ($A=$Ca and Sr) and $Ca_2MnMoO_6$ crystals lies between 0.8 and 1.2 eV, respectively.

## ACKNOWLEDGMENTS

We thank A. Paul and T. K. Pyne for technical assistance.

[1] J. M. D. Coey, M. Viret, and S. von Molnar, Adv. Phys. **48**, 167 (1999).
[2] *Colossal Magnetoresistive Oxides*, edited by Y. Tokura (Gordon and Breach, New York, 2000).
[3] N. F. Mott, *Metal-Insulator Transition*, 2nd ed. (Taylor and Francis, London, 1990).
[4] K.-I. Kobayashi, T. Kimura, H. Sawada, K. Terakura, and Y. Tokura, Nature (London) **395**, 677 (1998).
[5] M. T. Anderson, K. B. Greenwood, G. A. Taylor, and K. R. Poeppelmeier, Prog. Solid State Chem. **22**, 197 (1993).
[6] Y. Moritomo, Sh. Zhu, A. Machida, T. Akimoto, E. Nishibori, M. Takata, M. Sakata, and K. Ohoyama, J. Phys. Soc. Jpn. **69**, 1723 (2000).
[7] R. P. Borges, R. M. Thomas, C. Cullinant, J. M. D. Coey, R. Suryanarayanan, L. Ben-Dor, L. Pinsard-Gaudart, and A. Revcolevschi, J. Phys.: Condens. Matter **11**, L445 (1999).
[8] S. Roy, A. Kumar, D. D. Sharma, R. Cimino, S. Turchini, S. Zennaro, and N. Zema, Phys. Rev. Lett. **87**, 097204 (2001).
[9] D. D. Sharma, P. Mahadevan, T. Saha-Dasgupta, S. Roy, and A. Kumar, Phys. Rev. Lett. **85**, 2549 (2000).
[10] A. W. Sleight and J. F. Weiher, J. Phys. Chem. Solids **33**, 679 (1972).
[11] Y. Moritomo, Sh. Xu, A. Machida, T. Akimoto, E. Nishibori, M. Takata, and M. Sakata, Phys. Rev. B **61**, R7827 (2000).
[12] G. Blasse, Philips Res. Rep. **20**, 377 (1965); J. Inorg. Nucl. Chem. **27**, 993 (1965).
[13] H. Kawanaka, I. Hase, S. Toyama, and Y. Nishihara, J. Phys. Soc. Jpn. **68**, 2890 (1990); Physica B **281–282**, 518 (2000).
[14] T. Nakagawa, K. Yoshikawa, and S. Nomura, J. Phys. Soc. Jpn. **27**, 880 (1969).
[15] K.-I. Kobayashi, T. Okuda, Y. Tomioka, T. Kimura, and Y. Tokura, J. Magn. Magn. Mater. **218**, 17 (2000).
[16] R. I. Dass and J. B. Goodenough, Phys. Rev. B **63**, 064417 (2001).
[17] S. Roy, A. Kumar, S. Majumdar, E. V. Sampathkumaran, and D. D. Sharma, J. Phys.: Condens. Matter **13**, 607 (2001).
[18] R. Gangopadhyay, A. Dey, and S. Das, J. Appl. Phys. **87**, 2363 (2000).
[19] C. Ritter, M. R. Ibarra, L. Morellon, J. Blasco, J. Garcia, and J. M. D. Teresa, J. Phys.: Condens. Matter **12**, 8295 (2000).
[20] A. Arulraj, K. Ramesha, J. Gopalkrishnan, and C. N. Rao, J. Solid State Chem. **155**, 233 (2000).
[21] J. B. Philipp, P. Majewski, L. Alff, A. Erb, R. Gross, T. Graf, M. S. Brandt, J. Simon, T. Walther, W. Mader, D. Topwal, and D. D. Sharma, cond-mat/0306357.
[22] J.-S. Kang, H. Han, B. W. Lee, C. G. Olson, S. W. Han, K. H. Kim, J. I. Jeong, J. H. Park, and B. I. Min, Phys. Rev. B **64**, 024429 (2001).
[23] J. B. Torrance, P. Lacorre, A. I. Nazzal, E. J. Ansaldo, and ch. Niedermayer, Phys. Rev. B **45**, 8209 (1992); P. Lacorre, J. B. Torrance, J. Pannetier, A. I. Nazzal, P. W. Wang, and T. C. Huang, J. Solid State Chem. **91**, 225 (1991).
[24] H. Yanagihara, M. B. Salamon, Y. Lyanda-Geller, Sh. Zhu, and Y. Moritomo, Phys. Rev. B **64**, 214401 (2001).
[25] I. Mannari, Prog. Theor. Phys. **22**, 335 (1959).
[26] M. Itoh, I. Ohota, and Y. Inaguma, Mater. Sci. Eng., B **B41**, 55 (1996).
[27] N. F. Mott and E. A. Davis, *Electronic Processes in Non-crystalline Materials* (Oxford, Clarendon, 1979), pp. 32–34.

[28] B. I. Shklovskii and A. L. Efros, *Electronic Properties of Doped Semiconductors*, (Springer-Verlag, Berlin, 1984), p. 74.
[29] K. Maiti, N. Y. Vasanthacharya, and D. D. Sharma, J. Phys.: Condens. Matter **9**, 7507 (1997).
[30] *Thermoelectricity in Metallic Conductors*, edited by F. J. Blatt and P. A. Schroeder (Plenum Press, New York, 1977).
[31] N. F. Mott and H. Jones, *The Theory of the Properties of Metals and Alloys* (Dove, New York, 1958), p. 310.